Chem Rev Lett 6 (2023) 262-275

Research Article

Chemical Review and Letters
journal homepage: www.chemrevlett.com
ISSN (online): 2645-4947 (print) 2676-7279

Exploration of the mutual effects between cation–π and intramolecular hydrogen bond interactions in the different complexes of mesalazine with metal cations of alkali and alkaline-earth: A DFT study

Fahimeh Alirezapour [1, *], Marziyeh Mohammadi[2], Azadeh Khanmohammadi[1]

[1] Department of Chemistry, Payame Noor University (PNU), P.O.Box 19395-4697 Tehran, Iran
[2] Department of Chemistry, Faculty of Science, Vali-e-Asr University of Rafsanjan, Rafsanjan, Iran

ARTICLE INFO

Article history:
Received 7 September 2023
Received in revised form 30 September 2023
Accepted 6 October 2023
Available online 26 October 2023

Keywords:
Cation-π
Intramolecular hydrogen bond
DFT
AIM
NBO

ABSTRACT

The current investigation utilizes the density functional theory (DFT) approach to examine the interplay effects of the cation-π and intramolecular hydrogen bond (IMHB) interactions in the complexes created by the combination of mesalazine and metal cations (Li^+, Na^+, K^+, Be^{2+}, Mg^{2+}, and Ca^{2+}). The aim of this study is to estimate the topological properties through the use of the atoms in molecules (AIM) analysis. In addition, the charge transfer values will be determined using the natural bond orbital (NBO) analysis. The findings suggest that the coupling simultaneously diminishes the strength of the IMHB and enhances the interaction between the cation and the π-system. Furthermore, there is an increase in the strength of cation-π interactions as the charge-to-radius ratio of the cations increases. Conversely, we observe opposite results for the interactions involving IMHB. Finally, the utilization of frontier molecular orbitals is employed in the assessment of the conceptual parameters of DFT, including the energy gap, chemical hardness, and electronic chemical potential of the complexes.

1. Introduction

Mesalazine (MES), alternatively referred to as mesalamine or 5-aminosalicylic acid, is a pharmaceutical agent employed in the management of inflammatory bowel disorders, encompassing ulcerative colitis and Crohn's disease [1]. It is a drug that is specific to the intestines and belongs to the class of aminosalicylates. Following oral administration, it undergoes metabolism in the gastrointestinal tract and primarily displays its effects in that region [2]; as a result, the occurrence of adverse reactions diminishes. The structure and therapeutic properties of the MES diverge significantly from those of 4-aminosalicylic acid (or p-aminosalicylic acid). The mechanism by which MES operates when treating inflammatory bowel disease is currently undiscovered; however, its functionality is hypothesized to involve the regulation of chemical mediators involved in the inflammatory response, specifically prostaglandins and leukotrienes. The MES hinders the activity of the cyclooxygenase enzyme in the arachidonic acid cascade, consequently diminishing the synthesis of prostaglandins involved in inflammation [3-5].

The noncovalent interactions (NCIs) such as hydrogen bond, cation–π, anion–π, π–π, etc. have attracted the special attention of scientists due to their applications in science and technology [6, 7]. These interactions are very important in the chemical reactions, drug-receptor interactions, crystal engineering, protein folding, and regulation of biochemical processes [8, 9]. One of the most significant indicators of NCIs is the HB [10, 11]. The importance of HB in biological structure, function, and structural dynamics cannot be overstated. The HB is essential for life as it evolves on Earth [12]. The properties of X, Y and H (X–H···Y), substituent,

---

* Corresponding author.; e-mail: falirezapoor@pnu.ac.ir
https://doi.org/ 10.22034/CRL.2023.415348.1245

hybridization and solvation are the key factors that affect the nature of HB [13]. The cation–π interactions, as an additional cluster of NCIs, delineate the affinity between a positively charged ion and the planar surface of a chemical compound encompassing a conjugated system [14-16]. The cation-π interaction typically exhibits greater strength compared to other NCIs associated with the π-system, such as π-π and π-HB [14]. The significance of this interaction is contingent upon the nature of both the π-system and the cation participating in the interaction [17-19].

The interplay among NCIs in biological systems is important in areas of the supramolecular chemistry and molecular recognition [20]. The phenomenon of cation–π and HB interactions has been the subject of numerous investigations, exploring their mutual influences. In the 2021, Mohammadi et al. [21] conducted an evaluation on the impacts arising from the interplay of cation–π and intramolecular hydrogen bond interactions on the complexes formed by methyl salicylate with Li^+, Na^+, K^+, Be^{2+}, Mg^{2+}, Ca^{2+} cations. Khanmohammadi et al. [22] directed an examination into the impact of cation-π interactions on the potency and characteristics of the intra-molecular $O^{\cdots}H$ hydrogen bond within the orthohydroxy benzaldehyde compound, alongside a selection of mono- and divalent metal cations, including Li^+, Na^+, K^+, Be^{2+}, Mg^{2+} and Ca^{2+}. Also, the enhancing effect of the cation–π interaction on the intramolecular hydrogen bond in the acetaminophen complex was analyzed in 2020 [23].

There are several studies in evaluating the importance of interaction of metals with biomolecules [24-31]. The objective of this investigation is to examine the mutual influences between cation–π and IMHB interactions within the compounds created by the mesalazine medication and metal cations (Li^+, Na^+, K^+, Be^{2+}, Mg^{2+} and Ca^{2+}). For this purpose, the parent molecule (MES) and the benzene (BEN) compound with the aforementioned cations have been selected as a collection of benchmark points. The DFT calculations are used to analyze the energetic, geometric and spectroscopic parameters. In addition, the AIM and NBO analyses are applied to evaluate the topological parameters and charge transfer values, respectively. Finally, the frontier molecular orbitals (FMOs) are calculated to estimate the conceptual DFT parameters such as energy gap, global hardness, softness, electronic chemical potential, electrophilicity index and electronegativity of the considered complexes. We hope that our results can provide helpful information about the performance of these complexes in the discovery of compounds with new bioactive ligands.

2. Computational methodology

Quantum chemistry package Gaussian 0٩ [32] is utilized to perform the calculations in the present study. The structures are optimized with the ωB97XD functional and the 6-311++G(d,p) basis set [33] to evaluate the interaction between the species. This methodology incorporates the utilization of empirical atom-atom dispersion to implement a long-range correction [34–37]. Density functional theory [38] has been verified to be valid for studying the non-covalent complexes. Harmonic vibrational frequencies are estimated at the same level of theory. The absence of imaginary frequencies reveals that the studied complexes have particular local minima on the PES and are therefore stable. The calculation of the binding energy ($\Delta E_{ion-\pi}$) between the constituents involves the assessment of the disparity between the aggregate energy of the complexes and that of each individual monomer, as delineated below:

$$\Delta E_{ion-\pi} = E_{cation-\pi} - (E_{cation} + E_{\pi\text{-system}}) + E_{BSSE} \qquad (1)$$

where the total energy of the complexes, denoted as $E_{cation-\pi}$, can be expressed as the sum of the energies of the relaxed cations (E_{cation}) and the MES (or BEN) monomer ($E_{\pi\text{-system}}$). The E_{BSSE} is the basis set superposition error (BSSE) energy [39] applied to correct the binding energy. In order to more understanding about the nature of the interactions, the analysis of the AIM [40] is performed by the AIM2000 program [41]. For the selected configurations, the donor-acceptor energies and the charge transfer values are also estimated through the NBO analysis [42, 43]. In addition, the molecular orbital calculations such as the highest occupied molecular orbital (HOMO) and the lowest unoccupied molecular orbital (LUMO) energies are applied to evaluate the conceptual DFT parameters like softness (S), chemical hardness (η), electronic chemical potential (μ), electronegativity (χ) and electrophilicity index (ω). Finally, to predict the behavior and reactivity of the complexes, the electrostatic potential (ESP) distribution is exploited by the Multiwfn 3.6 program [44]. The analysis of ESP is typically conducted on the molecular radius of van der Waals (vdW), which is assessed at the 0.001 electrons/Bohr3 isodensity surfaces. Additionally, the vdW surface, which is visualized using the VMD 1.9.3 program [45], is demonstrated in terms of ESP.

3. Results and discussion

3.1. Energies

In this study, the DFT calculation is performed on the MES···M complexes (M = Li^+, Na^+, K^+, Be^{2+}, Mg^{2+}, Ca^{2+}) to investigate the interplay effects between cation-π and IMHB interactions. To compare the results, a set of reference points including the parent molecule (MES) and the benzene complexes (BEN···M) are also considered. The optimized structures of MES···M and BEN···M complexes are depicted in Scheme 1. The BSSE-corrected binding energies (ΔE_{BSSE}) at the ωB97XD/6-311++G(d,p) level of theory are given in Table 1. As exemplified in this Table, the inclination in absolute values of ΔE_{BSSE} for both MES and BEN complexes can be observed as $\pi\cdots Be^{2+} > \pi\cdots Mg^{2+} > \pi\cdots Ca^{2+} > \pi\cdots Li^+ > \pi\cdots Na^+ > \pi\cdots K^+$.

One of the key factors that is effective in binding energies is the charge-to-radius ratio (Q/r) of the cations as Be^{2+} (6.452) > Mg^{2+} (3.077) > Ca^{2+} (2.020) > Li^+ (1.667) > Na^+ (1.052) > K^+ (0.752). As observed, there is a direct relationship between the binding energies and the charge-to-radius ratio of the cations with a correlation coefficient (R^2) equal to 0.9744 (Scheme S1 in the supplementary section). Based on the obtained results, the values of binding energies (ΔE_{BSSE}) for the MES and BEN complexes are in the ranges of -18.89 to -235.90 and -17.64 to -216.15 kcal mol^{-1}, respectively. As the results show, the ΔE_{BSSE} values for the MES···M complexes are higher than those of the BEN···M series (see Table 1). This indicates that the coupling of cation–π and IMHB increases the strength of the cation–π interactions.

The Espinosa method [46] is also applied to estimate the IMHB energy of the MES complexes. There exists a significant correlation between the HB energy (E_{HB}) and the potential energy of electrons at the critical point of the bond (V_{bcp}), which can be expressed as $E_{HB} = 1/2\ V_{(bcp)}$ [46-48]. The results in Table 1 show that the increasing trend of HB energies is as $\pi\cdots K^+ > \pi\cdots Na^+ > \pi\cdots Li^+ > \pi\cdots Ca^{2+} > \pi\cdots Mg^{2+} > \pi\cdots Be^{2+}$. As it is clear, an inverse relationship exists between the E_{HB} values and the charge-to-radius ratio of the cations in the related complexes. Inspection of results in Table 1 shows that the presence of cation–π interaction diminishes the HB strength. This means that the HB energy for the MES complexes is lower than its monomer. Scheme S2 reveals the correlation between the HB energies and the binding energies with a correlation coefficient (R^2) of 0.9311.

3.2. Molecular geometry

The optimized geometrical parameters such as bond length and angle are given in Table 1. The distance among the ions and the middle of the aromatic ring ($d_{\pi\cdots M}$) is the most important structural parameter in determining the cation–π interactions. The results show that the $d_{\pi\cdots M}$ obviously changes with the strengthening of the cation–π interaction. Examining the results in Table 1 shows that the trend in the $d_{\pi\cdots M}$ values for alkaline-earth and alkali complexes is as $\pi\cdots Ca^{2+} > \pi\cdots Mg^{2+} > \pi\cdots Be^{2+}$ and $\pi\cdots K^+ > \pi\cdots Na^+ > \pi\cdots Li^+$, respectively. Our data reveal that, in most cases, the coupling of the IMHB and cation–π interactions reduces the values of $d_{\pi\cdots M}$ in the MES complexes relative to their corresponding values in the BEN ones. This indicates that the presence of HB increases the strength of the cation-π interactions.

To evaluate the HB character in the presence of cation-π interactions, the geometrical parameters of the O–H···O unit are also investigated. The HB distances and their corresponding angles are key factors that affect the HB strength [49]. The geometrical parameters of the complexes are collected in Table 1. As seen in this Table, the $d_{H\cdots O}$ values decrease in the following order: $\pi\cdots Be^{2+} > \pi\cdots Mg^{2+} > \pi\cdots Ca^{2+} > \pi\cdots Li^+ > \pi\cdots Na^+ > \pi\cdots K^+$, which in accordance with the calculated E_{HBs}. In order to understand the effect of cation–π interaction on the HB strength, the bond lengths and angles of MES complexes are compared with those of their monomer. According to the obtained results, the lowest values of $d_{H\cdots O}$ and d_{O-H} and the highest values of θ_{OHO} belong to the parent molecule (MES). This means that the presence of the cation-π interaction weakens the HB strength. It is also worth mentioning that the $d_{H\cdots O}$ and d_{O-H} values correlate well with the binding energies (see Scheme S3).

3.3. Spectroscopic study

The strength of the NCIs can also be evaluated by calculating the stretching frequencies. These quantities are strongly under the influence of cation–π interactions strength. As shown in Table 1, the order of the stretching frequencies of the cation–π contact ($\nu_{\pi\cdots M}$) for alkaline-earth and alkali complexes is as $\pi\cdots Be^{2+} > \pi\cdots Mg^{2+} > \pi\cdots Ca^{2+}$ and $\pi\cdots Li^+ > \pi\cdots Na^+ > \pi\cdots K^+$, respectively. For the studied complexes, the comparison of the calculated binding energies with the $\nu_{\pi\cdots M}$ values shows a direct relationship between them (see Table 1). As the results show, in most cases, the values of $\nu_{\pi\cdots M}$ for the MES complexes are higher than the BEN series. This indicates that the cation–π interaction is strengthened in the MES complexes with respect to those of BEN. According to these data, the coupling of IMHB and cation–π interactions increases the values of $\nu_{\pi\cdots M}$.

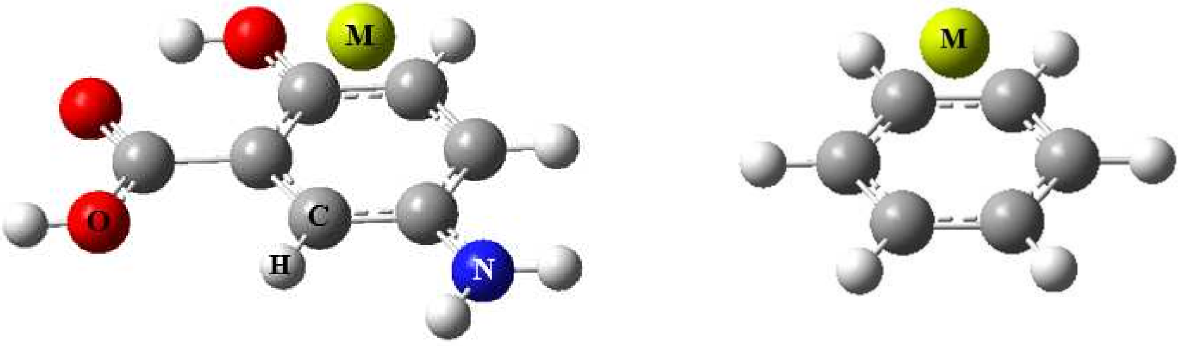

(a)

(b)

Scheme 1. Molecular structures of MES···M (a) and BEN···M (b) complexes (M = Li^+, Na^+, K^+, Be^{2+}, Mg^{2+}, Ca^{2+}).

Table 1. The BSSE-corrected binding and IMHB energies (ΔE_{BSSE} and E_{HB}, in kcal mol^{-1}), the geometrical parameters (bond lengths (d), in Å and bond angles (θ), in °) and spectroscopic data (ν, in cm^{-1}) of complexes calculated at the ωB97XD/6-311++G(d,p) level of theory.

	ΔE_{BSSE}	$d_{\pi\cdots M}$	$\nu_{\pi\cdots M}$	E_{HB}	$d_{O\text{-}H}$	$d_{H\cdots O}$	θ_{OHO}	$\nu_{O\text{-}H}$
BEN···Li^+	-35.98	1.957	342.8	–	–	–	–	–
BEN···Na^+	-23.87	2.495	179.7	–	–	–	–	–
BEN···K^+	-17.64	2.898	135.1	–	–	–	–	–
BEN···Be^{2+}	-216.15	1.290	613.7	–	–	–	–	–
BEN···Mg^{2+}	-108.78	1.956	357.3	–	–	–	–	–
BEN···Ca^{2+}	-77.16	2.367	244.5	–	–	–	–	–
MES	–	–	–	-11.29	0.974	1.786	144.0	3620.0
MES···Li^+	-36.66	1.955	334.1	-10.93	0.976	1.795	141.6	3581.9
MES···Na^+	-24.75	2.500	191.2	-11.05	0.976	1.792	142.0	3591.5
MES···K^+	-18.89	2.890	115.7	-11.10	0.976	1.791	142.2	3591.9
MES···Be^{2+}	-235.90	1.331	663.0	-10.07	0.984	1.816	137.6	3481.7
MES···Mg^{2+}	-120.89	1.951	366.9	-10.34	0.981	1.810	138.6	3522.9
MES···Ca^{2+}	-87.51	2.331	295.7	-10.78	0.980	1.798	139.3	3529.7

In the O–H···O unit, the O–H stretching frequency ($\nu_{O–H}$) is the most significant vibrational mode that affects the nature of the HB. The $\nu_{O–H}$ values of the complexes are listed in Table 1. It is well-established that the formation of the X–H···Y bond in conventional HBs causes the X–H bond to expand and the corresponding X–H stretching vibration to shift to a lower frequency [50]. As shown in Table 1, the presence of cation-π interactions reduces the $\nu_{O\text{-}H}$ values of the MES complexes relative to its monomer. This indicates the weakening of the HB strength in the related complexes. The results also display that the red shift of the O–H stretching frequencies of MES complexes relative to its monomer (Δν) is as π···Be^{2+} (138) >

$\pi\cdots Mg^{2+}$ (97) > $\pi\cdots Ca^{2+}$ (90) > $\pi\cdots Li^{+}$ (38) > $\pi\cdots Na^{+}$ (29) > $\pi\cdots K^{+}$ (28 cm^{-1}). Furthermore, as depicted in Scheme S4, the ν_{O-H} values correlate to binding energies while their correlation coefficient (R^2) is equal to 0.9291.

3.4. AIM analysis

In order to more understanding about the nature of the interaction between species, the topological parameters of electron density (ρ), its Laplacian ($\nabla^2\rho$), total energy density of electrons (H), and kinetic (G) and potential (V) electron energy densities in term of bond critical points (BCPs) are investigated. The interactions property can be categorized as a function of H_{BCP} and $\nabla^2\rho_{BCP}$ [51, 52]. The strong interactions have the covalent character ($\nabla^2\rho_{BCP} < 0$ and $H_{BCP} < 0$), the medium interactions are partially covalent ($\nabla^2\rho_{BCP} > 0$ and $H_{BCP} < 0$) and the weak interactions are mainly electrostatic ($\nabla^2\rho_{BCP} > 0$ and $H_{BCP} > 0$). The results of AIM analysis are reported in Table 2. As shown in this Table, the interaction between cations and the π-system is electrostatic with the values of small $\rho(r)_{\pi\cdots M}$, $\nabla^2\rho(r)_{\pi\cdots M} > 0$ and $H(r)_{\pi\cdots M} > 0$. This means that the electronic charges are depleted in the interatomic path, which indicates the nature of closed-shell interactions in these systems. In the case of Be^{2+} complexes with the values of $\nabla^2\rho(r)_{\pi\cdots M} > 0$ and $H(r)_{\pi\cdots M} < 0$, the interaction is partially covalent. The type of cations and the nature of the π-system are two factors that determine the BCPs formed in the complexes through their molecular graphs (see Scheme 2). As revealed in this Scheme, the existence of cation-π interactions in the considered complexes is confirmed by the corresponding bond path between the cations and each carbon atom of the aromatic ring.

Comparing the values of $\rho(r)_{\pi\cdots M}$ with the binding energies of the complexes shows a direct relationship between them (see Tables 1 and 2). The correlation coefficient (R^2) for the dependency of ΔE_{BSSE} versus $\rho(r)_{\pi\cdots M}$ is equal to 0.9881 (see Scheme S5). The results in Table 2 display that the trend in values of $\rho(r)_{\pi\cdots M}$ is as $\pi\cdots Be^{2+}$ > $\pi\cdots Mg^{2+}$ > $\pi\cdots Ca^{2+}$ > $\pi\cdots Li^{+}$ > $\pi\cdots Na^{+}$ > $\pi\cdots K^{+}$. Obviously, the coupling of the cation–π and IMHB interactions increases the $\rho(r)_{\pi\cdots M}$ values in the MES complexes compared to the BEN, which emphasizes the presence of a stronger cation-π interaction. The character of NCIs can also be assessed by the -G/V ratio [53, 54]: for $-G/V \geq 1$, the interaction is mainly electrostatic, while for $0.5 < -G/V < 1$, its partially covalent character is defined. As seen in Table 2, the $-G/V_{\pi\cdots M}$ values obtained for the complexes are greater than 1, which reveals their electrostatic nature. On the other hand, the $-G/V_{\pi\cdots M}$ values for the Be^{2+} complexes indicate that the interaction is partially covalent.

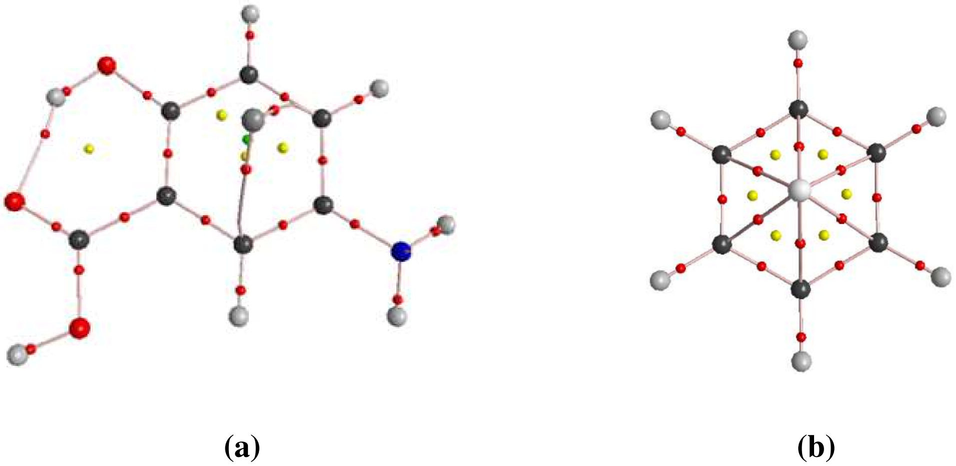
(a) (b)

Scheme 2. Molecular graphs commonly acquired from AIM analysis for MES···M (a) and BEN···M (b) complexes.

The topological properties of HB critical points are collected in Table 2. The presence of HB interactions is verified by the formation of BCPs between groups of the proton-donating and proton-accepting objects (see Scheme 2a). The HBs are classified into three categories: the weak HBs, characterized by $\nabla^2\rho(r) > 0$ and $H(r) > 0$; the medium HBs, described by $\nabla^2\rho(r) > 0$ and $H(r) < 0$; and the strong HBs, depicted by $\nabla^2\rho(r) < 0$ and $H(r) < 0$ [55]. Based on the results calculated in Table 2, the values of $\nabla^2\rho(r)_{H\cdots O} > 0$ and $H(r)_{H\cdots O} < 0$ obtained in the complexes indicate that they may be placed in category of the medium HBs. As shown in

Table 2, the increasing trend of $\rho(r)_{H\cdots O}$ values is as $\pi\cdots K^+ > \pi\cdots Na^+ > \pi\cdots Li^+ > \pi\cdots Ca^{2+} > \pi\cdots Mg^{2+} > \pi\cdots Be^{2+}$, which is in agreement with the calculated HB energies. According to the results, the coexistence of IMHB and cation–π interactions decreases the $\rho(r)_{H\cdots O}$ values at the HB critical points relative to its monomer, indicating the weakening of the HB strength. Scheme S6 reveals a good correlation between the values of $\rho(r)_{H\cdots O}$ and the binding energies. The results also show that the complexes analyzed in this study are partially covalent in nature, because their $-G/V_{H\cdots O}$ ratio is between 0.5 and 1 (see Table 2).

To investigate the nature of the NCIs between species, the reduce density gradient (RDG) study is also performed using the Multiwfn program [44]. The binding nature and recognition of the interacting regions in the complexes are evaluated with the color-filled RDG plots. The regions of strong attractive, weak and repulsive interactions are marked using blue, green and red colors, respectively. The iso-surface maps of the RDG for the $MES\cdots Mg^{2+}$ and $MES\cdots Li^+$ complexes are depicted in Scheme 3. As observed in this Scheme, the interaction between the ions and the aromatic ring center for the $MES\cdots Mg^{2+}$ and $MES\cdots Li^+$ complexes is shown by the blue and green colors, respectively, which confirms the strength of cation-π interactions in these systems. Furthermore, the interaction region marked by blue color indicates the formation of a hydrogen bond between the proton donor and proton acceptor in the O–H···O unit. The red regions display strong steric effects in the complexes.

Table 2. The chosen topological parameters of electron density (in a. u.) acquired through AIM analysis.

	π···M					HB				
	ρ(r)	$\nabla^2\rho(r)$	H(r)	V(r)	-G/V	ρ(r)	$\nabla^2\rho(r)$	H(r)	V(r)	-G/V
$BEN\cdots Li^+$	0.0138	0.0738	0.0039	-0.0107	1.361	–	–	–	–	–
$BEN\cdots Na^+$	0.0088	0.0419	0.0024	-0.0056	1.428	–	–	–	–	–
$BEN\cdots K^+$	0.0083	0.0322	0.0017	-0.0046	1.367	–	–	–	–	–
$BEN\cdots Be^{2+}$	0.0574	0.1943	-0.0083	-0.0652	0.872	–	–	–	–	–
$BEN\cdots Mg^{2+}$	0.0259	0.1138	0.0030	-0.0225	1.132	–	–	–	–	–
$BEN\cdots Ca^{2+}$	0.0220	0.0774	0.0015	-0.0164	1.091	–	–	–	–	–
MES	–	–	–	–	–	0.0385	0.1291	-0.0018	-0.0360	0.949
$MES\cdots Li^+$	0.0146	0.0759	0.0038	-0.0113	1.338	0.0377	0.1260	-0.0016	-0.0348	0.953
$MES\cdots Na^+$	0.0097	0.0451	0.0025	-0.0062	1.404	0.0379	0.1269	-0.0017	-0.0352	0.951
$MES\cdots K^+$	0.0096	0.0374	0.0019	-0.0057	1.328	0.0381	0.1274	-0.0018	-0.0354	0.950
$MES\cdots Be^{2+}$	0.0614	0.2154	-0.0095	-0.0729	0.870	0.0357	0.1185	-0.0012	-0.0321	0.962
$MES\cdots Mg^{2+}$	0.0287	0.1253	0.0027	-0.0259	1.104	0.0363	0.1211	-0.0013	-0.0329	0.960
$MES\cdots Ca^{2+}$	0.0244	0.0866	0.0013	-0.0190	1.070	0.0374	0.1241	-0.0017	-0.0343	0.952

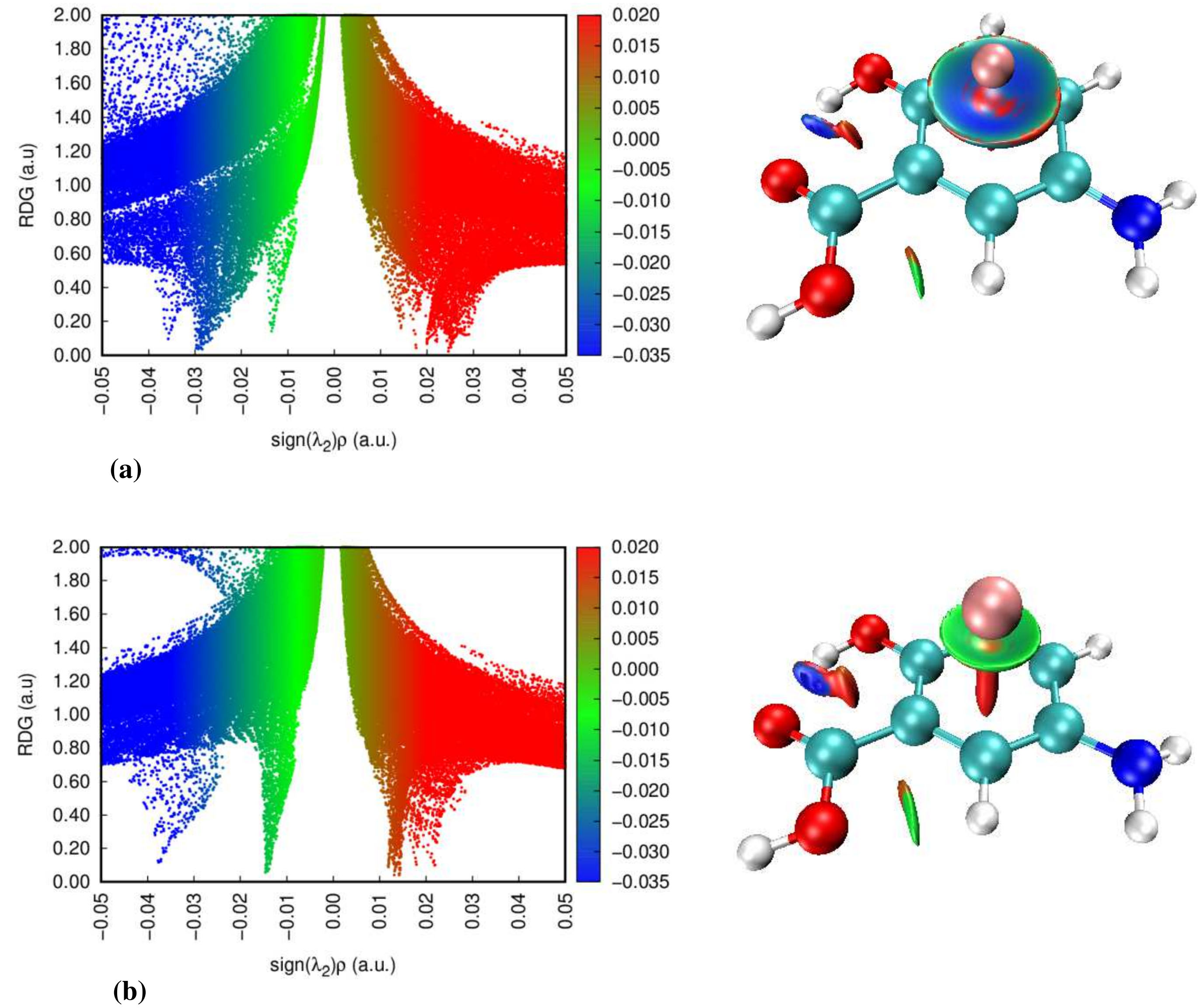

Scheme 3. Reduced density gradient iso-surface maps of the MES···Mg^{2+} (a) and MES···Li^{+} (b) complexes.

3.5. NBO analysis

The natural bond orbital analysis [42, 56] considers the orbital interactions and the charge transfer values in the complexes. The results of the NBO analysis including the second-order perturbation energy ($E^{(2)}$), charge transfer (Δq_{CT}) and occupation number of NBOs are given in Table 3. The obtained results show that the most significant interaction formed between cations and π-system is $\pi_{C=C} \rightarrow LP^*_M$. In the NBO analysis of the studied structures, the charge transfer between the bonding orbitals of benzene C=C (as electron donor) and the antibonding lone pair of cations (as electron acceptor) has a particular importance. Inspection of results in Table 3 shows that the trend in the $E^{(2)}$ values of the complexes is π···Be^{2+} > π···Mg^{2+} > π···Ca^{2+} > π···Li^{+} > π···Na^{+} > π···K^{+}, which have greater values in the MES complexes compared to BEN ones. This indicates that the presence of the HB ring increases the cation–π interaction strength.

The charge transfer ($\Delta q_{(CT1)}$) values of the complexes are also listed in Table 3. The $\Delta q_{(CT1)}$ of the species is calculated from the difference between the atomic charge of the ions in the free state and the complexed. The data demonstrate that the existence of HB enhances the amounts of $\Delta q_{(CT1)}$ for the divalent complexes in comparison with their respective magnitudes in BEN, while the opposite process is observed for the monovalent structures. In addition, as shown in Table 3, the values of $\Delta q_{(CT1)}$ and the charge transfer energies ($E^{(2)}$) are in good agreement with each other.

In the analysis of HB systems using NBO methodology, the transfer of charge between the lone pairs of the proton acceptor ($LP_{(O)}$) and the antibonds of the proton donor ($\sigma^*_{(O–H)}$) emerges as a paramount aspect. The findings obtained from the NBO analysis conducted for the $LP_{(O)} \rightarrow \sigma^*_{(O–H)}$ interaction can be found in Table 3. As seen in this Table, the donor–acceptor energies decrease in the following order: $\pi\cdots K^+ > \pi\cdots Na^+ > \pi\cdots Li^+ > \pi\cdots Ca^{2+} > \pi\cdots Mg^{2+} > \pi\cdots Be^{2+}$. As the results show, the value of $E^{(2)}$ for the MES complexes is lower than that of the parent molecule. The presence of the IMHB and cation–π interactions, as determined from the acquired data, exhibits a diminishing effect on the strength of the HB. Scheme S7 depicts the ΔE_{BSSE} dependency on the values of $E^{(2)}$ corresponding to HB with a correlation coefficient (R^2) equal to 0.928.

The NBO analysis is additionally utilized to examine the alteration in charge on the oxygen atom (q_O) implicated in HB (see Table 3). As illustrated in this Table, the interaction between the cations and the MES system leads to a decrease in the $|q_O|$ values compared to its corresponding monomer (q_O = -0.344). The values of charge transfer ($\Delta q_{(CT2)}$) are evaluated from the difference between the atomic charges of the oxygen in free state and complexed with an equation as: $\Delta q_{(CT2)} = q_O\,(\text{complex}) - q_O\,(\text{monomer})$. As Table 3 demonstrates, the divalent and monovalent complexes are correlated with the highest and lowest magnitudes of $|\Delta q_{(CT2)}|$, respectively. This suggests that the charge transfer may be a helpful quantity in elucidating the strength of these interactions.

Table 3. The values of $E^{(2)}$ correspond to $\pi_{(C=C)} \rightarrow LP^*_{(M)}$ and $LP_{(O)} \rightarrow \sigma^*_{(O–H)}$ interactions (in kcal mol^{-1}), occupation numbers of donor (ON_D) and acceptor (ON_A) orbitals, oxygen atomic charges ($q_{(O)}$) and the charge transfers ($\Delta q_{(CT)}$, in e).

	π···M interaction				HB interaction				
	$\pi_{(C=C)} \rightarrow LP^*_{(M)}$				$LP_{(O)} \rightarrow \sigma^*_{(O–H)}$				
	$E^{(2)}$	$ON_{\pi(C=C)}$	$ON_{LP^*(M)}$	$\Delta q_{(CT1)}$	$E^{(2)}$	$ON_{LP(O)}$	$ON_{\sigma^*(O–H)}$	$q_{(O)}$	$\Delta q_{(CT2)}$
BEN···Li$^+$	4.17	1.6475	0.0312	0.423	–	–	–	–	–
BEN···Na$^+$	0.94	1.6581	0.0108	0.164	–	–	–	–	–
BEN···K$^+$	0.54	1.6612	0.0053	0.046	–	–	–	–	–
BEN···Be^{2+}	50.22	1.5119	0.2382	1.443	–	–	–	–	–
BEN···Mg^{2+}	13.86	1.6075	0.0925	0.956	–	–	–	–	–
BEN···Ca^{2+}	7.27	1.6276	0.0553	0.494	–	–	–	–	–
MES	–	–	–	–	14.25	1.8541	0.0367	-0.344	–
MES···Li$^+$	5.54	1.7334	0.0281	0.373	13.49	1.8474	0.0361	-0.271	-0.073
MES···Na$^+$	1.15	1.7393	0.0089	0.147	13.66	1.8490	0.0364	-0.284	-0.060
MES···K$^+$	0.71	1.7388	0.0046	0.019	13.77	1.8497	0.0365	-0.292	-0.052
MES···Be^{2+}	71.8	1.6375	0.1894	1.523	11.88	1.8319	0.0350	-0.188	-0.156
MES···Mg^{2+}	15.76	1.6022	0.1123	1.062	12.33	1.8379	0.0351	-0.215	-0.129
MES···Ca^{2+}	9.54	1.7316	0.0486	0.535	13.05	1.8411	0.0364	-0.231	-0.113

3.6. HOMO–LUMO analysis

The kinetic stability and chemical reactivity of compounds are also evaluated by frontier molecular orbitals (FMOs) [57, 58]. The HOMO and LUMO correspond to the capacity of donating and gaining electrons, respectively [59]. The discrepancy between the HOMO and LUMO is defined as the band gap (E_g) in chemistry, which plays an important role in the stability [60]. The HOMO and LUMO plots for the Li^+ complexes are illustrated in Scheme 4. The reactivity descriptors known in terms of softness (S), chemical hardness (η) [61], electronic chemical potential (μ) [62], global electrophilicity power (ω) [63] and electronegativity (χ) [64] are computed according to the following equations:

$$\eta = \frac{(E_{LUMO} - E_{HOMO})}{2} \tag{2}$$

$$\mu = -\chi = \frac{(E_{LUMO} + E_{HOMO})}{2} \tag{3}$$

$$S = \frac{1}{2\eta} \tag{4}$$

where the terms E_{LUMO} and E_{HOMO} are used to describe the lowest unoccupied molecular orbital and the highest occupied molecular orbital energies, respectively. The electrophilicity index (ω) is ascribed to the electrophilic characteristic of the compounds and is formulated in the following style:

$$\omega = \frac{\mu^2}{2\eta} \tag{5}$$

The dependence of a molecule's chemical hardness and softness on the energy gap is a notable phenomenon. Hard molecules have a large E_g, high stability and low reactivity, while the reverse results are defined for soft molecules. Analysis of the results in Table 4 indicates that the highest value of hardness is related to the Be^{2+} complex, while the lowest value corresponds to the Mg^{2+} one. Therefore, the maximum values of stability and reactivity belong to the Be^{2+} and Mg^{2+} complexes, respectively.

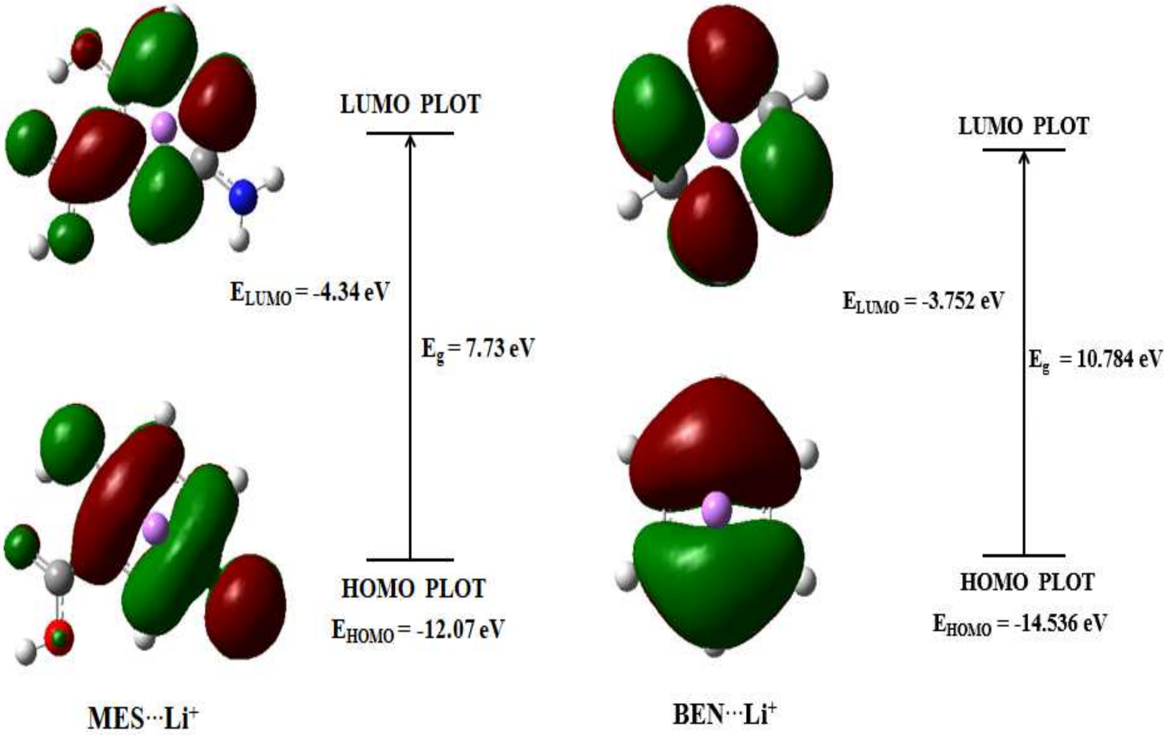

Scheme 4. The molecular orbital diagrams of MES···Li^+ and BEN···Li^+ complexes determined using the wB97XD/6-311++G(d,p) level of theory.

Table 4. Values of the HOMO and LUMO energies (E_{HOMO}, E_{LUMO}), energy gap (E_g), chemical hardness (η), softness (S), electronic chemical potential (μ), electronegativity (χ) and electrophilicity index (ω).

	E_{HOMO} (eV)	E_{LUMO} (eV)	E_g (eV)	η (eV)	S (eV^{-1})	μ (eV)	χ (eV)	ω (eV)
BEN···Li^+	-14.536	-3.752	10.784	5.392	0.093	-9.144	9.144	7.754
BEN···Na^+	-13.802	-3.692	10.110	5.055	0.099	-8.747	8.747	7.568
BEN···K^+	-13.397	-3.206	10.191	5.096	0.098	-8.301	8.301	6.762
BEN···Be^{2+}	-22.011	-10.606	11.405	5.702	0.088	-16.308	16.308	23.320
BEN···Mg^{2+}	-20.058	-10.730	9.328	4.664	0.107	-15.394	15.394	25.405
BEN···Ca^{2+}	-19.138	-9.136	10.002	5.001	0.100	-14.137	14.137	19.981
MES	-7.592	0.082	7.674	3.837	0.130	-3.755	3.755	1.838
MES···Li^+	-12.071	-4.344	7.726	3.863	0.129	-8.208	8.208	8.719
MES···Na^+	-11.618	-3.910	7.708	3.854	0.130	-7.764	7.764	7.821
MES···K^+	-11.377	-3.658	7.719	3.859	0.130	-7.517	7.517	7.322
MES···Be^{2+}	-17.980	-9.930	8.049	4.025	0.124	-13.955	13.955	24.194
MES···Mg^{2+}	-16.586	-10.110	6.478	3.239	0.154	-13.347	13.347	27.497
MES···Ca^{2+}	-16.109	-8.952	7.157	3.578	0.140	-12.530	12.530	21.939

According to the results of Table 4, all the complexes considered in this study are stable. This can be contributed to the obtained negative μ values. There is a meaningful relationship between the chemical potential and the electronegativity as: $\chi = -\mu$. Our data display that the best electron acceptors are the divalent complexes with higher values of χ. The reactivity of the complexes can also be predicted by the electrophilicity index. The electrophilicity of the complexes can be evaluated by the η and μ parameters. The performing a chemical reaction in the compounds with the values of lower η and higher |μ| is more appropriate; because the electrons transfer is easier in them [65]. The results of Table 4 show the maximum and minimum the electrophilicity values for the divalent and monovalent complexes, respectively.

Our findings in Table 4 also indicate that in the presence of HB, the E_g, η and χ values for the MES complexes are lower than their corresponding values in the BEN, while the S, μ and ω indices show the higher values for these complexes. On the other hand, the coexistence of the cation-π and IMHB interactions leads to an increase in the values of E_g, η, χ and ω, and a decrease in the indices of S and μ for the MES complexes compared to its monomer (except for Mg^{2+} and Ca^{2+} complexes). Obviously, with the exception of the ω index, the reverse results are observed for these descriptors in both the interactions. This means that the interactions influence each other in the opposite directions.

3.7. Electrostatic potential (ESP)

The ESP is another indicator that provides a visual depiction of chemically active sites and the relative reactivity of atoms. The donating and accepting tendencies of the NCIs can be attributed to the most positive ESP ($V_{S,max}$) and the most negative ESP ($V_{S,min}$), respectively. The $V_{S,max}$ and $V_{S,min}$ values are calculated using the Multiwfn program [44]. The electron density isosurfaces for the MES···Li^+ complex and its monomer are shown in Scheme 5. In the MES monomer, the $V_{S,min}$ value of -30.28 kcal mol^{-1} (global minimum on the surface) is closer to the oxygen atom; its large negative value is due to the lone pairs on this atom. The $V_{S,max}$ value of +55.47 kcal mol^{-1} (global maximum on the surface) is in the vicinity of the positively charged H; its large amount is due to the existence of oxygen, which absorbs a great deal of electrons from H.

In the MES···Li$^+$ complex, the $V_{S,min}$ is +38.63 kcal mol^{-1}, which is closer to the oxygen atom of the carboxyl group; it is the most beneficial site for the positively charged atoms and plays the role of the most probable acceptor. On the other hand, the $V_{S,max}$ value is observed on top of the Li$^+$ cation with a value of +291.67 kcal mol^{-1}, which is the most favorable place for the negatively charged species and acts as the most possible donor. These observations obviously describe the reason why carboxyl groups can form HB. They also display that cations should be ideal sites for electrophilic reactions.

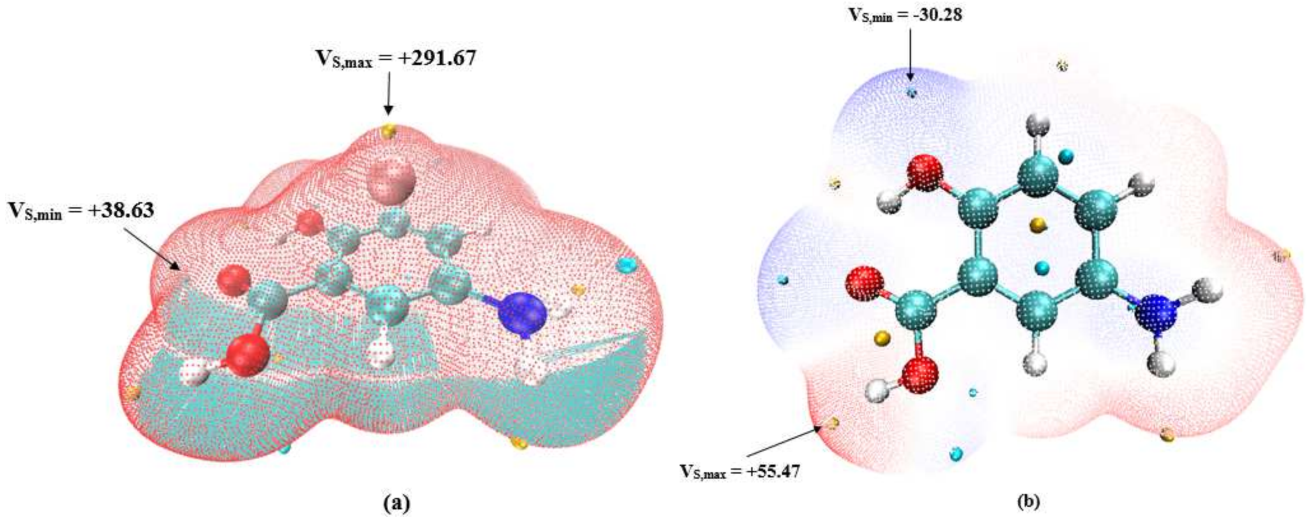

Scheme 5. Molecular electrostatic surface potentials of the MES···Li$^+$ complex (a) and the MES monomer (b) mapped on their corresponding 0.001 au electron density isosurface along with the $V_{S,max}$ and $V_{S,min}$ values measured in units of kcal mol^{-1}.

4. Conclusion

The current investigation assesses the mutual effects of cation-π and IMHB interactions on MES complexes containing Li$^+$, Na$^+$, K$^+$, Be^{2+}, Mg^{2+} and Ca^{2+} cations. This study aims to examine the geometrical parameters, binding energies, topological properties, and charge transfer analysis in order to compare their results with those of BEN complexes and the MES molecule, which serve as a reference point. Several relationships can be observed among the energetic, geometric, and topological variables. Based on the acquired findings, it can be inferred that the coupling simultaneously not only diminishes the intensity of the IMHB but also enhances the interaction between cations and π-electron systems. Our findings also demonstrate that the strength of the cation–π interactions enhances with increasing the charge-to-radius ratio of the cations, while the opposite results are observed for the IMHB interactions. These outcomes are also confirmed by AIM and NBO analyses. The findings from the analysis of molecular orbitals reveal that the quantum molecular descriptors exhibit contrasting outcomes for both the cation-π and HB interactions, with the exception of ω. This suggests that the impact of HB on the cation-π interaction differs from the influence of the cation-π interaction on HB. Therefore, the relationship between these omnipresent NCIs in biological systems may hold significance in numerous domains of supramolecular chemistry.

Acknowledgements

The authors wish to thank the Payame Noor University, Tehran, Iran for its support.

Supplementary data

Supplementary data to this article can be found online at doi:

References

[1] M. Iacucci, S. de Silva, S. Ghosh, Mesalazine in inflammatory bowel disease: A trendy topic once again? *Can. J. Gastroenterol.*, 24 (2010) 127–133.

[2] G. Rubin, A.P.S. Hungin, D. Chinn, A.D. Dwarakanath, L. Green, J. Bates, Long-term aminosalicylate therapy is under-used in patients with ulcerative colitis: A cross-sectional survey. *Aliment. Pharmacol. Ther.*, 16 (2002) 1889–1893.

[3] O.H. Nielsen, K. Bukhave, J. Elmgreen, I. Ahnfelt-Ronne, Inhibition of 5-lipoxygenase pathway of arachidonic acid metabolism in human neutrophils by sulfasalazine and 5-aminosalicylic acid. *Dig. Dis. Sci.*, 32 (1987) 577-582.

[4] Y.R. Mahida, C.E. Lamming, A. Gallagher, A.B. Hawthorne, C.J. Hawkey, 5-Aminosalicylic acid is a potent inhibitor of interleukin-1 beta production in organ culture of colonic biopsy specimens from patients with inflammatory bowel disease. *Gut.*, 32 (1991) 50–54.

[5] G.C. Kaiser, F. Yan, D.B. Polk, Mesalamine blocks tumor necrosis factor growth inhibition and nuclear factor kappa B activation in mouse colonocytes. *Gastroenterol.*, 116 (1999) 602–609.

[6] P. Hubza, K. Moller-Dethlefs, Non-covalent Interactions: Theory and Experiment, Royal Society of Chemistry, Cambridge (2010).

[7] S. Scheiner, Non-covalent Forces, Springer, Heidelberg (2015).

[8] E.A. Meyer, R.K. Castellano, F. Diederich, Interactions with aromatic rings in chemical and biological recognition. *Angew. Chem. Int. Ed.*, 42 (2003) 1210–1250.

[9] K. Muller-Dethlefs, P. Hobza, Noncovalent interactions: a challenge for experiment and theory. *Chem. Rev.*, 100 (2000) 143–168.

[10] C.L. Perrin, J.B. Nielson, "Strong" hydrogen bonds in chemistry and biology. *Annu. Rev. Phys. Chem.*, 48 (1997) 511-544.

[11] G.R. Desiraju, Hydrogen bridges in crystal engineering: interactions without borders. *Acc. Chem. Res.*, 35 (2002) 565–573.

[12] G.A. Jeffrey, W. Saenger, Hydrogen Bonding in Biology and Chemistry, Springer-Verlag, Berlin (1991).

[13] R. Wysokinski, D.C. Biennko, D. Michalska, T.Z. Huyskens, Theoretical study of the interaction between cytosine and hydrogen peroxide. *Chem. Phys.*, 315 (2005) 17-26.

[14] J.C. Ma, D.A. Dougherty, The cation- π interaction. *Chem. Rev.*, 97 (5) (1997) 1303-1324.

[15] Y. An, S.E. Wheeler, Cation–π interactions, In Encyclopedia of Inorganic and Bioinorganic Chemistry, Wiley & Sons (2011).

[16] D.A. Dougherty, The cation-π interaction. *Acc. Chem. Res.*, 46 (2013) 885–893.

[17] J.B. Nicholas, P.B. Hay, D.A. Dixon, Binding Enthalpies for Alkali Cation−Benzene Complexes Revisited. *J. Phys. Chem. A*, 104 (2000) 11414-11419.

[18] D. Feller, A complete basis set estimate of cation-π bond strengths: Na^+(ethylene) and Na^+(benzene). *Chem. Phys. Lett.,* 322 (2000) 543-548.

[19] A. Pullman, G. Berthier, R. Savinelli, Components of the interaction energy of benzene with Na^+ and methylammonium cations. *J. Mol. Struct. (Theochem)*, 537 (2001) 163-172.

[20] C.A. Hunter, J.K.M. Sanders, The nature of π–π interactions. *J. Am. Chem. Soc.*, 112 (1990) 5525–5534.

[21] M. Pirgheibi, M. Mohammadi, A. Khanmohammadi, Density functional theory study of the interplay between cation–π and intramolecular hydrogen bonding interactions in complexes involving methyl salicylate with Li^+, Na^+, K^+, Be^{2+}, Mg^{2+}, Ca^{2+} cations. *Comput. Theor. Chem.*, 1198 (2021) 113172.

[22] A. Khanmohammadi, F. Ravari, The influence of cation-π interactions on the strength and nature of intramolecular O···H hydrogen bond in orthohydroxy benzaldehyde compound. *Phys. Chem. Res.*, 5 (2017) 57–68.

[23] M. Mohammadi, A. Khanmohammadi, Theoretical investigation on the non-covalent interactions of acetaminophen complex in different solvents: study of the enhancing effect of the cation–π interaction on the intramolecular hydrogen bond. *Theor. Chem. Acc.*, 139 (2020) 141.

[24] R. Ghiasi, M. Rahimi, R. Ahmadi, Quantum-chemical investigation into the complexation of titanocene dichloride with C_{20} and $M^+@C_{20}$ (M^+ = Li, Na, K) cages. *J. Struct. Chem.*, 61 (2020) 1681–1690.

[25] M. Monajjemi, R. Ghiasi, M.A. Seyed Sadjadi, Metal-stabilized rare tautomers: N4 metalated cytosine (M = Li^+, Na^+, K^+, Rb^+ and Cs^+), theoretical views. *Appl. Organomet. Chem.*, 17 (2003) 635-640.

[26] R. Ghiasi, M. Monajjemi, F. Asadian, H. Pasdar, Theoretical investigation of the interaction of uracil and mono hydrated uracil - water complexes with alkali metals. *J. Chem. Res.*, 2004 (2004) 445-449.

[27] M. Monajjemi, R. Ghiasi, S. Ketabi, H. Passdar, F. Mollaamin, A theoretical study of metal-stabilised rare tautomers stability: N4 metalated cytosine (M = Be^{2+}, Mg^{2+}, Ca^{2+}, Sr^{2+}, and Ba^{2+}) in gas phase and different solvents. *J. Chem. Res.*, 2004 (2004) 11-18.

[28] R. Ghiasi, M. Monajjemi, Theoretical study of interaction of alkaline earth metal with C4O4 2- and C4S4 2-: Structure, electronic properties and aromaticity. *J. Sulphur Chem.*, 28 (2007) 537-546.

[29] R. Ghiasi, M. Monajjemi, Theoretical study of the dihydrogen bonded HMH¨HB≡NH and HMH¨HN≡BH complexes (M=Be, Mg and Ca): Properties and structures. *Main Group Chem.*, 7 (2008) 123-131.

[30] R. Ghiasi, Theoretical insights into the properties of the XY≡YX¨M^{n+} complexes (X = H, F, Cl; Y = C, Si; M = alkaline and alkaline earth metals). *J. Struct. Chem.*, 51 (2010) 204-210.

[31] R. Ghiasi, Theoretical investigation of the structure and properties of $H_2B{=}NH_2\cdots M^{n+}$, $HB{\equiv}NH\cdots M^{n+}$, and Borazine$\cdots M^{n+}$ complexes (M = Alkaline and Earth Alkaline Metals). *Russ. J. Phys. Chem. A*, 85 (2011) 2148-2155.

[32] M.J. Frisch, G.W. Trucks, H.B. Schlegel, G.E. Scuseria, M.A. Robb, J.R. Cheese-man, G. Scalmani, V. Barone, B. Mennucci, G.A. Petersson, H. Nakatsuji, M. Caricato,

X. Li, H.P. Hratchian, A.F. Izmaylov, J. Bloino, G. Zheng, J.L. Son-nenberg, M. Hada, M. Ehara, K. Toyota, R. Fukuda, J. Hasegawa, M. Ishida, T. Nakajima, Y. Honda, O. Kitao, H. Nakai, T. Vreven, J.A. Montgomery Jr, J.E. Peralta, F. Ogliaro, M.J. Bearpark, J. Heyd, E.N. Brothers, K.N. Kudin, V.N. Staroverov, R. Kobayashi, J. Normand, K. Raghavachari, A.P. Rendell, J.C. Bu-rant, S.S. Iyengar, J. Tomasi, M. Cossi, N. Rega, N.J. Millam, M. Klene, J.E. Knox, J.B. Cross, V. Bakken, C. Adamo, J. Jaramillo, R. Gomperts, R.E. Stratmann, O. Yazyev, A.J. Austin, R. Cammi, C. Pomelli, J.W. Ochterski, R.L. Martin, K. Mo-rokuma, V.G. Zakrzewski, G.A. Voth, P. Salvador, J.J. Dannenberg, S. Dapprich, A.D. Daniels, Ö. Farkas, J.B. Foresman, J.V. Ortiz, J. Cioslowski, D.J. Fox, Gaussian 09, Gaussian, Inc., Wallingford, CT, USA (2009).

[33] M.J. Frisch, J.A. Pople, J.S. Binkley, Self-consistent molecular orbital methods 25. Supplementary functions for Gaussian basis sets. *J. Chem. Phys.*, 80 (1984) 3265-3269.

[34] H. Iikura, T. Tsuneda, T. Yanai, K. Hirao, A long-range correction scheme for generalized-gradient-approximation exchange functionals. *J. Chem. Phys.*, 115 (2001) 3540.

[35] A. Savin, H.J. Flad, Density functionals for the Yukawa electron-electron interaction. *Int. J. Quantum Chem.*, 56 (1995) 327–332.

[36] J.D. Chai, M. Head-Gordon, Systematic optimization of long-range corrected hybrid density functionals. *J. Chem. Phys.*, 128 (2008) 084106.

[37] J.D. Chai, M. Head-Gordon, Long-range corrected hybrid density functionals with damped atom–atom dispersion corrections. *Phys. Chem. Chem. Phys.*, 10 (2008) 6615-6620.

[38] A.J. Cohen, P.M. Sanchez, W. Yang, Insights into Current Limitations of Density Functional Theory. *Science* 321 (2008) 792-794.

[39] A. Hassanpour, M.R. Poor Heravi, A. Khanmohammadi, Electronic sensors for alkali and alkaline earth cations based on Fullerene‑ C60 and silicon doped on C60 nanocages: a computational study. *J. Mol. Model.*, 28 (2022) 148.

[40] R.F.W. Bader, Atoms in Molecules: A Quantum Theory, Oxford University Press, Oxford (1990).

[41] F. Biegler König, J. Schönbohm, Update of the AIM2000-program for atoms in molecules. *J. Comput. Chem.*, 23 (2002) 1489–1494.

[42] J.P. Foster, F. Weinhold, Natural hybrid orbitals. *J. Am. Chem. Soc.*, 102 (1980) 7211-7218.

[43] (a) J.E. Carpenter, F. Weinhold, Analysis of the geometry of the hydroxymethyl radical by the “different hybrids for different spins” natural bond orbital procedure”. *J. Mol. Struct. (Theochem)*, 169 (1988) 41-62; (b) A.E. Reed, R.B. Weinstock, F. Weinhold, Natural population analysis. *J. Chem. Phys.*, 83 (1985) ٧٣٥.

[44] T. Lu, F. Chen, Multiwfn: a multifunctional wavefunction analyzer. *J. Comput. Chem.*, 33 (2012) 580-592.

[45] E. Abdulkareem Mahmood, M.R. Poor Heravi, A. Khanmohammadi, S. Mohammadi‑ Aghdam, A.G. Ebadi, S. Habibzadeh, DFT calculations, structural analysis, solvent effects, and non‑ covalent interaction study on the para‑ aminosalicylic acid complex as a tuberculosis drug: AIM, NBO, and NMR analyses. *J. Mol. Model.*, 28 (2022) 297.

[46] E. Espinosa, E. Molins, Retrieving interaction potentials from the topology of the electron density distribution: the case of hydrogen bonds. *J. Chem. Phys.*, 113 (2000) 5686–5694.

[47] M. Mohammadi, A. Khanmohammadi, Theoretical investigation on the non‑ covalent interactions of acetaminophen complex in different solvents: study of the enhancing effect of the cation–π interaction on the intramolecular hydrogen bond. *Theor. Chem. Account.*, 139 (2020) 141.

[48] Y.A. Abramov, On the possibility of kinetic energy density evaluation from the experimental electron-density distribution. *Acta. Crystallogr. A*, 53 (1997) 264–272.

[49] M. Mohammadi, F. Alirezapour, A. Khanmohammadi, DFT calculation of the interplay effects between cation–π and intramolecular hydrogen bond interactions of mesalazine drug with selected transition metal ions (Mn^{+}, Fe^{2+}, Co^{+}, Ni^{2+}, Cu^{+}, Zn^{2+}). *Theor. Chem. Account.*, 140 (2021) 104.

[50] M. Pirgheibi, M. Mohammadi, A. Khanmohammadi, A comparative study of interplay effects between the cation-π and intramolecular hydrogen bond interactions in the various complexes of methyl salicylate with Mn^{+}, Fe^{2+}, Co^{+}, Ni^{2+}, Cu^{+}, and Zn^{2+} cations. *Struct. Chem.*, 32 (2021) 1529-1539.

[51] R.F.W. Bader, Atoms in Molecules. *Acc. Chem. Res.*, 18 (1985) 9-15.

[52] (a) D. Bijani, R. Ghiasi, S. Baniyaghoob, DFT investigation of stability, electronic and optical properties of coordination of C20 corannulene to $Fe(CO)_4$. *Inorg. Chem. Commun.*, 153 (2023) 110793; (b) H. Asadzadeh, R. Ghiasi, M. Yousefi, S. Baniyaghoob, Electronic, Structural, and Optical Properties of $Fe(CO)_4[X_{12}Y_{12}]$ (X = B or Al, Y = N or P) Complexes: A Computational Investigation. *Russ. J. Inorg. Chem.*, 68 (2023). DOI: 10.1134/S0036023623600338; (c) H. Asadzadeh, R. Ghiasi, M. Yousefi, S. Baniyaghoob, C-PCM study on the electronic and optical properties of $Fe(CO)_4B_{12}N_{12}$ complexes. *Main Group Chem.*, 22 (2023) 31-41; (d) S. Shayanmehr, R. Ghiasi, B. Mirza, B. Mohtat, Hydrogen Adsorption and Storage on Palladium-Functionalized C_{20} Bowl and $C_{20}H_{10}$ Bowl Molecule Including Hydrogen Saturation. *J. Struct. Chem.*, 63 (2022) 1399-1408; (e) A. Solgi, R. Ghiasi, S. Baniyaghoob, PCM, ETS-NOCV, and CDA investigations of interactions of a Cycloplatinated Thiosemicarbazone as Antiparasitic and Antitumor Agents with C_{20} Nano-Cage. *Int. J. Nano Dimens.*, 14 (2023) 219-226; (f) R. Ghiasi, A. Valizadeh, Computational Investigation of Interaction of

a Cycloplatinated Thiosemicarbazone as Antitumor and Antiparasitic Agents with $B_{12}N_{12}$ Nano-Cage. *Results Chem.*, 5 (2023) 100768; (g) R. Ghiasi, R. Tale, V. Daneshdoost, A. Yousefi Siavoshani, The nature of the interactions between $B_{12}N_{12}$ and inorganic aromatic molecules ($B_3N_3H_6$, $B_3P_3H_6$, $B_3O_3H_3$, $B_3S_3H_3$). *Russ. J. Inorg. Chem.*, 68 (2023) 1-8; (h) R. Ghiasi, N. Sadeghi, Evolution of the interaction between C_{20} cage and $Cr(CO)_5$: A solvent effect, QTAIM and EDA investigation. *J. Theor. Comput. Chem.*, 16 (2017) 1750007.

[53] R.D. Parra, J. Ohlssen, Cooperativity in intramolecular bifurcated hydrogen bonds: an ab initio study. *J. Phys. Chem. A*, 112 (2008) 3492–3498.

[54] M. Zioˈłkowski, S.J. Grabowski, J. Leszczynski, Cooperativity in hydrogen bonded interactions: ab initio and "atoms in molecules" analyses. *J. Phys. Chem. A*, 110 (2006) 6514–6521.

[55] I. Rozas, I. Alkorta, J. Elguero, Behavior of ylides containing N, O and C atoms as hydrogen bond acceptors. *J. Am. Chem. Soc.*, 122 (2000) 11154-11161.

[56] (a) M. Khademi Shamami, R. Ghiasi, M. Daghighi Asli, The Analysis of Electronic Structures, NBO, EDA, and QTAIM of trans-$(H_3P)_2(\eta^2\text{-BH4})W(\equiv C\text{-para-}C_6H_4X)(CO)$ Complexes. *J. Chin. Chem. Soc.*, 64 (2017) 369-378; (b) A. Valizadeh, R. Ghiasi, Theoretical approach to the molecular structure, chemical reactivity, molecular orbital analysis, spectroscopic properties (IR, UV, NMR), and NBO analysis of deferiprone. *J. Struct. Chem.*, 58 (2017) 1307-1317; (c) S.H. Saraf, R. Ghiasi, QTAIM, ELF and LOL Investigations on trans-$(NHC)PtI_2(\text{para-}NC_5H_4X)$ Complexes. *J. Chem. Res.*, 44 (2020) 482–486; (d) G. Ghane Shalmani, R. Ghiasi, A. Marjani, EDA, CDA and QTAIM Investigations in the $(\text{para-}C_5H_4X)\ Ir(PH_3)_3$ Iridabenzene Complexes. *Russ. J. Phys. Chem. B*, 15 (2021) S6–S13; (e) R. Ghiasi, S. Abdolmohammadi, S. Moslemizadeh, Quantum Mechanical Study of Substituent Dependence on the Structure, Spectroscopic (^{13}C, ^{1}H NMR and UV), NBO, Hyperpolarizability and HOMO-LUMO Analysis of $Ru(NHC)_2Cl_2(=CH\text{-p-}C_6H_4X)$ Complexes. *J. Chin. Chem. Soc.*, 62 (2015) 898-905.

[57] K. Fukui, T. Yonezaw, H. Shingu, A molecular orbital theory of reactivity in aromatic hydrocarbons. *J. Chem. Phys.*, 20 (1952) 722–725.

[58] L.H. Mendoza-Huizar, C.H. Rios-Reyes, Chemical reactivity of atrazine employing the Fukui function. *J. Mex. Chem. Soc.*, 55 (2011) 142–147.

[59] K. Fukui, Role of Frontier Orbitals in Chemical Reactions. *Science*, 218 (1982) 747-754.

[60] B. Kosar, C. Albayrak, Spectroscopic investigations and quantum chemical computational study of (E)-4 -methoxy-2-[(p-tolylimino) methyl] phenol. *Spectrochim. Acta. A*, 78 (2011) 160–167.

[61] M. Mohammadi, A. Khanmohammadi, Molecular structure, QTAIM and bonding character of cation–π interactions of mono and divalent metal cations (Li^+, Na^+, K^+, Be^{2+}, Mg^{2+} and Ca^{2+}) with drug of acetaminophen. *Theor. Chem. Account.*, 138 (2019) 101.

[62] F. Alirezapour, Y. Keshavarz, A.A. Minaeifar, A. Khanmohammadi, Structural analysis and electronic properties of transition metal ions (Ni^{2+}, Fe^{2+}, Mn^+ and Co^+) with psoralen biomolecule as an anticancer drug. *J. Organomet. Chem.*, 986 (2023) 122606.

[63] M. Mohammadi, M. mahinian, A. Khanmohammadi, Theoretical Study of Stability and Electronic Characteristics in Various Complexes of Psoralen as an Anticancer Drug in Gas Phase, Water and CCl_4 Solutions. *Chem. Res. Chinese Universities*, 38 (2022) 1414-1424.

[64] F. Alirezapour, A. Khanmohammadi, The effect of cation–π interactions on the stability and electronic properties of anticancer drug Altretamine: a theoretical study. *Acta Cryst.*, C76 (2020) 982-991.

[65] M.R. Jalali Sarvestani, R. Ahmadi, Investigating the Complexation of a recently synthesized phenothiazine with Different Metals by Density Functional Theory. *Int. J. New. Chem.*, 4 (2017) 101-110.